

Research Paper

Casein-Coated Fe₅C₂ Nanoparticles with Superior r₂ Relaxivity for Liver-Specific Magnetic Resonance Imaging

Taku A. Cowger¹, Wei Tang¹, Zipeng Zhen¹, Kai Hu², David E. Rink¹, Trever J. Todd¹, Geoffrey D. Wang¹, Weizhong Zhang¹, Hongmin Chen¹, Jin Xie^{1,3,✉}

1. Department of Chemistry, University of Georgia, Athens, GA 30602, USA
2. Department of Chemistry, Wuhan University, Wuhan, Hubei, China
3. Bio-Imaging Research Center, the University of Georgia, Athens, Georgia 30602, USA.

✉ Corresponding author: E-mail: jinxie@uga.edu

© 2015 Ivyspring International Publisher. Reproduction is permitted for personal, noncommercial use, provided that the article is in whole, unmodified, and properly cited. See <http://ivyspring.com/terms> for terms and conditions.

Received: 2015.05.02; Accepted: 2015.07.10; Published: 2015.08.09

Abstract

Iron oxide nanoparticles have been extensively used as T₂ contrast agents for liver-specific magnetic resonance imaging (MRI). The applications, however, have been limited by their mediocre magnetism and r₂ relaxivity. Recent studies show that Fe₅C₂ nanoparticles can be prepared by high temperature thermal decomposition. The resulting nanoparticles possess strong and air stable magnetism, suggesting their potential as a novel type of T₂ contrast agent. To this end, we improve the synthetic and surface modification methods of Fe₅C₂ nanoparticles, and investigated the impact of size and coating on their performances for liver MRI. Specifically, we prepared 5, 14, and 22 nm Fe₅C₂ nanoparticles and engineered their surface by: 1) ligand addition with phospholipids, 2) ligand exchange with zwitterion-dopamine-sulfonate (ZDS), and 3) protein adsorption with casein. It was found that the size and surface coating have varied levels of impact on the particles' hydrodynamic size, viability, uptake by macrophages, and r₂ relaxivity. Interestingly, while phospholipid- and ZDS-coated Fe₅C₂ nanoparticles showed comparable r₂, the casein coating led to an r₂ enhancement by more than 2 fold. In particular, casein coated 22 nm Fe₅C₂ nanoparticle show a striking r₂ of 973 mM⁻¹s⁻¹, which is one of the highest among all of the T₂ contrast agents reported to date. Small animal studies confirmed the advantage of Fe₅C₂ nanoparticles over iron oxide nanoparticles in inducing hypointensities on T₂-weighted MR images, and the particles caused little toxicity to the host. The improvements are important for transforming Fe₅C₂ nanoparticles into a new class of MRI contrast agents. The observations also shed light on protein-based surface modification as a means to modulate contrast ability of magnetic nanoparticles.

Key words: iron carbides, magnetic nanoparticles, magnetic resonance imaging, casein, surface modification, macrophages

Introduction

Liver cancer remains a major cause of mortality worldwide. In the United States, liver cancer is estimated to be diagnosed in more than 35,600 new patients in 2014 and cause 24,500 deaths [1]. The five-year survival rate is 27% and 42% for regional and localized tumors, respectively, but the rate is dropped to only 18% for liver cancer that has metastasized [2]. This status underscores the significance of

early diagnosis of liver cancer. Liver-specific magnetic resonance imaging (MRI) is one of the most extensively used methods in detection of hepatocellular diseases and tumor metastasis from other organs [3-7]. To improve detection accuracy, roughly 30-40% of the scans are performed with the assistance of either T₁ (spin-lattice) or T₂ (spin-spin) contrast agents [8-10]. So far, the most commonly used T₂ contrast

agents are iron oxide nanoparticles (IONPs) [11, 12]. IONPs are administered prior to a MRI scan and are taken up by the K pffer cells in the liver. The particles cause signal decrease on a T_2 -weighted image, producing contrast against lesions (e.g. a tumor) that are less abundant of the resident macrophages thereby improving the diagnosis sensitivity and accuracy [13]. However, clinically used IONP formulations, such as Feridex and Resovist, exhibit moderate contrast ability due to their mediocre magnetizations (~60-70 emu/g) [14-16]. Over the years, researchers have endeavored to synthesize nanoparticles made of higher magnetization materials such as Co [17], Fe [18], and FePt [19]. The resulting nanoparticles, however, have been often associated with issues including rapid oxidation [20], unstable magnetization in the air [21], harsh and often hazardous synthesis conditions [22], and high toxicity [23], and these drawbacks dim their perspectives of clinical translation.

Very recently, the Hou group and we reported the synthesis of iron carbide (Fe_5C_2) nanoparticles [15, 24]. Fe_5C_2 nanoparticles exhibit a high magnetization (~140 emu/g), relatively low toxicity, air stability, and facile synthesis [24]; more importantly, the high magnetization translates to r_2 relaxivity that is 2-3 folds higher than IONPs [15]. These findings suggest a great potential of Fe_5C_2 nanoparticles as an alternative T_2 contrast agent. In our previous studies, only 20 nm Fe_5C_2 nanoparticles were investigated [15]. It is postulated that the size of Fe_5C_2 nanoparticles may have an impact on their cellular uptake, magnetization, r_2 relaxivity, circulation half-lives [14,25], and therefore affecting their role as a liver contrast agent. These, however, have not been studied yet.

As-synthesized Fe_5C_2 particles inherit a thin shell of iron oxide from the synthesis [24]. This means that the surface modification methods previously developed for IONPs can be borrowed to modify Fe_5C_2 nanoparticles. These include ligand addition with amphiphilic ligands such as PEGylated phospholipids [25] and surface exchange with iron-philic molecules such as 2,3-dimercaptosuccinic acid (DMSA) [26] and zwitterion-dopamine-sulfonate (ZDS) [27]. In addition, protein based surface modification approaches that are more recently developed by us [28, 29] and others [30-32] are expected to be applicable to Fe_5C_2 nanoparticles. The surface coating may affect particles' interaction with the biological milieu [33], which has always been a topic of interest in nanoparticle developments, including the recent attention on protein corona of nanoparticles [31]. The coating may also affect the r_2 relaxivity of nanoparticles, but the topic has been much less studied, probably due to the relatively minor impact observed previously [34]. However, recent studies by Huang et al. showed that the r_2

relaxivity of IONPs can be increased by as much as ~2.5 fold when using casein as coating material [30], suggesting a bigger role surface coatings, and in particular protein-based surface coatings, can play in engineering T_2 contrast agents. Whether the coating effect can be modulated to further enhance the r_2 of Fe_5C_2 nanoparticles is worthy of investigations.

In the present study, we modified the previously reported synthetic approach and we prepared three sizes of Fe_5C_2 nanoparticles (5, 14, and 22 nm). These nanoparticles were then coated with PEGylated phospholipid, ZDS, or casein and the resulting conjugates were compared for their hydrodynamic size, macrophage uptake, toxicity, and r_2 relaxivity. Significant size and surface effects were observed, especially to the r_2 of the particles. In particular, the casein-coated 22 nm Fe_5C_2 nanoparticles show an extraordinary r_2 of 973 $mM^{-1}s^{-1}$ (on the basis of Fe), making it one of the highest among all the reported T_2 contrast agents to date [35]. In small animal studies, we found that casein-coated 22 nm Fe_5C_2 nanoparticles can induce at least 2.5 fold greater hypointensity to the liver than IONPs. These observations confirm the promise of Fe_5C_2 nanoparticles as novel T_2 contrast agents for liver imaging. In addition, the study sheds light on the great potential of modulating coatings for enhanced r_2 of magnetic nanoparticles.

Methods

Preparation of Fe_5C_2 Nanoparticles

Fe_5C_2 NPs were synthesized using a previously published protocol with minor modifications [15]. All of the chemical were from Sigma-Aldrich unless specified otherwise. For 22 nm Fe_5C_2 nanoparticle synthesis, 7.5 g of octadecylamine (ODA) and 56 mg of cetyltrimethylammonium bromide (CTAB) was added to a four-neck flask. The flask was purged with Ar gas and the temperature was increased to 393 K. 0.25 mL (3.6 mmol) of $Fe(CO)_5$ was added to the reaction mixture and the temperature was raised to 453 K to induce oxidation of $Fe(CO)_5$. After 10 min, the temperature was further raised to 693 K and maintained at the temperature for 10 min. The reaction system was then cooled to room temperature. The raw product was dissolved in a hexane/ethanol mixture and centrifuged for 10 min at 7500 rpm (6,174 g). This step was repeated for 6 times for the particles to be purified and the residual CTAB removed. For particles of larger and smaller sizes, the amount of $Fe(CO)_5$ added was doubled (7.2 mmol) and halved (1.8 mmol), respectively. The nanoparticles synthesized above were characterized by TEM (FEI Tecnai 20), dynamic light scattering (DLS, Malvern Zetasizer Nano S90), and X-ray diffraction (XRD, Bruker D8

Advanced X-ray diffractometer, Cu source).

Surface Modification Using Phospholipid

The as-synthesized Fe_5C_2 nanoparticles (1 mg/mL) were dried and redissolved in 1 mL CHCl_3 . ~60 μL of DSPE-PEG-COOH (10 mg/mL, Avanti Polar Lipids, Inc.) was added dropwise to the solution during stirring. The solution was left to stir for 1 hr and the solvent was evaporated off. The dried product was dispersed in deionized water with sonication and purified by centrifugation (6,174 g for 5 min) [15].

Surface Modification Using Zwitterion Dopamine Sulfonate (ZDS)

In a similar fashion to the previous modification, 50 mg of ZDS in 2 mL DMSO was added to a 4 mL CHCl_3 solution containing ~10 mg/mL Fe_5C_2 until the solution showed visible emulsion. The solution was then isolated by centrifugation (6,174 g for 10 min). The collected product was redispersed in water and centrifuged for 3 times to remove residual DMSO.

Surface Modification Using Casein

To prepare an aqueous solution of Fe_5C_2 particles, a solution of Fe_5C_2 in CHCl_3 was mixed with a preheated solution of excess glucose in DMF and refluxed for 1 hr. The resulting solution was then precipitated by ethanol and centrifuged (6,174 g for 10 min) and the process was repeated for three times. The purified product was redispersed in water. To prepare the casein addition, 100 mg of casein was treated with 0.01 M NaOH to form a soluble base in water. At a molar ratio of particle:casein at 1:200, the two mixtures were added to a flask and mixed for 4 hrs at room temperature. After 4 hrs, a 0.4% solution of glutaraldehyde (glutaraldehyde:casein 1:2) was dropwise added and the mixture was stirred for 1 hr at room temperature. The final product was purified by centrifugation and re-dissolved in water.

MRI Phantom Study

To analyze the relaxivities of these nanoparticles, a MRI phantom study was run. Nanoparticles at different concentrations were dispersed in 1% agarose gel in 300 μL tubes. The tubes were scanned on a 7T Varian small animal MRI system. T_2 -weighted fast spin echo images were obtained using the following parameters: TR = 2,000 ms; TE = 20, 40, 60, 80, and 100 ms; ETL = 8; field-of-view (FOV) = 40 mm \times 80 mm; slice thickness = 1 mm.

Cell Toxicity

1×10^4 RAW264.7 cells were placed in each well of a 96-well plate. After 24 hr incubation, Fe_5C_2 nanoparticles of varying concentrations (0 - 100 μg Fe/mL) were added and the incubation lasted for 4

hrs. The culture medium was removed after 4 hrs and replenished with fresh medium. Standard MTT assay was performed 24 hrs later to determine the cell viability.

Cell Uptake

1×10^6 RAW264.7 cells (murine macrophages) were placed in each of the three 2-well incubation chambers 24 hrs prior to the uptake study. Fe_5C_2 nanoparticles were added (0 - 100 μg Fe/mL) and incubated with the cells for 4 hrs. After incubation, the cells were washed using PBS. The cells were fixed with cold 95% ethanol for 15 min. Prussian blue staining was used to stain Fe while the nuclei of cells were stained with Nuclear Fast Red (Sigma-Aldrich). The slides were imaged on an optical microscope (Olympus X71). For quantitative analysis, the cells after incubation were collected and lysed by nitric acid (pH = 5.0, 72 hrs). The Fe content was determined by inductively coupled plasma mass spectrometry (ICP-MS) and the result was divided by cell count. Cells that had been incubated with casein-coated Fe_5C_2 nanoparticles were also collected for MRI phantom studies. The parameters were the same as those described above.

in vivo MRI

All the animal studies conform to the Guide for the Care and Use of Laboratory Animals published by the National Institutes of Health, USA, and a protocol approved by the Institutional Animal Care and Use Committee (IACUC), University of Georgia. Normal athymic nude mice were used for the *in vivo* imaging studies. The mice were anesthetized with isoflurane and tail-vein injected with casein-coated Fe_5C_2 or Fe_3O_4 nanoparticles at a dose of 2.5 mg Fe/kg ($n = 3$). Fe_3O_4 nanoparticles were Ocean Nanotech and were surface coated with casein. From T_2 -weighted fast spin echo images were obtained on a 7T Varian small animal system prior to as well as 1 hr and 4 hrs after the particle injection. The scan parameters were the following: TR = 2500 ms, TE = 40 ms, field-of-view (FOV) = 40 mm \times 80 mm, matrix size = 2562 and, thickness = 2 mm. After the 4 hr scan, the mice were sacrificed and their liver, kidneys, and spleen were excised and frozen in OCT (optimal cutting temperature compound) gel at -80 °C. The tissue blocks were cryo-sectioned into 8 μm slices and fixed in 10% formalin solutions for 25 min. The slides were rinsed with PBS carefully and immersed in a mixture of 20% HCl solution and 10% $\text{K}_4[\text{Fe}(\text{CN})_6] \cdot 3\text{H}_2\text{O}$ for 20 min. After washing by PBS, the slices were then counterstained with Fast Red solution for 5 min then washed again with PBS.

Results

Nanoparticle Synthesis and Characterization

Fe_5C_2 nanoparticle synthesis was similar to a previously published protocol [24]. Briefly, $\text{Fe}(\text{CO})_5$ was added to a Ar-purged mixture of octadecylamine and cetyltrimethylammonium bromide (CTAB) and the solution was heated up to the boiling point to induce $\text{Fe}(\text{CO})_5$ oxidation and carbonization [24]. In order to tune the size of these nanoparticles, the amount of the $\text{Fe}(\text{CO})_5$ precursor was varied. More specifically, we doubled and halved the amount of $\text{Fe}(\text{CO})_5$ previously used to yield Fe_5C_2 nanoparticles of relatively large and small sizes (Table 1). The nanoparticle size was determined by transmission electron microscopy (TEM, Figure 1A-C). All of the particles display a core-shell structure, with the shell about 1 nm in depth. The overall particle sizes are 5, 14, and 22 nm, respectively. The dynamic light scattering (DLS) results overall agree with the TEM measurements albeit slightly larger (Figure 1D and Table 1); the difference was attributed to the organic coating on the particle surface that is invisible under TEM. X-ray diffraction (XRD) analysis confirmed that the majority of the particles were $\theta\text{-Fe}_5\text{C}_2$ (JCPDS ID: 00-036-1248, Figure S1).

Surface modification

The as-synthesized Fe_5C_2 nanoparticles cannot

be dispersed in water. To make them water soluble, we used three surface modification methods. These include 1,2-distearoyl-sn-glycero-3-phosphoethanolamine-N-[carboxy(polyethylene glycol)-2000] (DSPE-PEG-COOH), which had used in our previous study [15]. The other two are ZDS-based ligand exchange and casein-based protein adsorption, which were proven to be successful to modify IONPs [30, 36]. The three strategies were all efficient to render Fe_5C_2 nanoparticles with good aqueous stability but the hydrodynamic sizes of the resulting formulations are varied. Taking 22 nm Fe_5C_2 nanoparticles for instance, ZDS, which is a small molecule, minimally affects the overall particle size (22.4 ± 1.4 nm, Figure 1E, Table 1, and Figure S2A&B). Phospholipid and casein coatings, on the other hand, significantly increased the hydrodynamic sizes to 35.3 ± 5.3 nm and 44.9 ± 6.5 , respectively (Figure 1E, Table 1, and Figure S2C&D). The nanoparticles were also stable in PBS containing 10% fetal bovine serum (FBS), showing no aggregation for over 1 week (Figure S3).

Table 1: TEM and DLS analysis results of Fe_5C_2 nanoparticles.

Shell (nm)	TEM results			DLS results	
	Core (nm)	Total (nm)	PL (nm)	ZDS (nm)	Casein (nm)
~1	2.7 ± 0.8	4.8 ± 0.9	12.1 ± 1.7	8.2 ± 0.6	16.8 ± 2.7
~1	11.4 ± 2.1	14.3 ± 2.3	23.2 ± 2.1	13.1 ± 0.2	32.4 ± 3.3
~1	19.5 ± 3.2	22.0 ± 3.4	35.3 ± 5.3	22.4 ± 1.4	44.9 ± 6.5

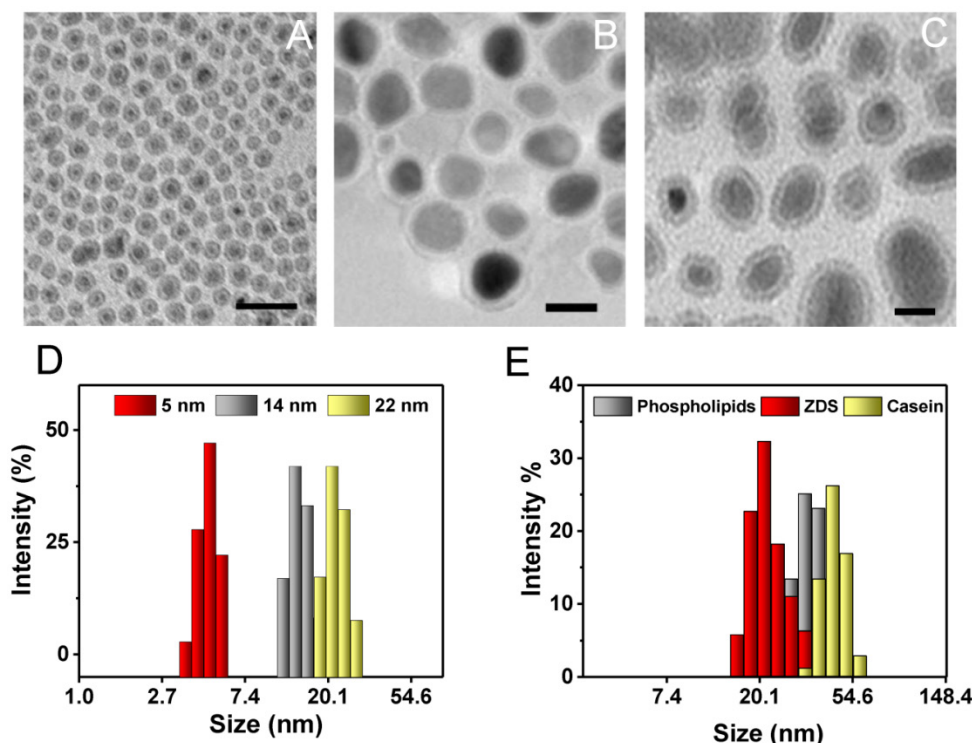


Figure 1: Characterization of Fe_5C_2 nanoparticles. A-C) TEM images of 5 nm (A), 14 nm (B), and 22 nm (C) Fe_5C_2 nanoparticles. The particle sizes were tuned by varying the amount of $\text{Fe}(\text{CO})_5$ precursor used for synthesis. Scale bars: 20 nm. D) DLS analysis of as-synthesized Fe_5C_2 nanoparticles of three sizes. E) DLS analysis of 22 nm Fe_5C_2 nanoparticles coated with phospholipids, ZDS, or casein.

Size and surface effects on r_2 relaxivity

We next assessed the r_2 relaxivities of all the nine Fe_5C_2 formulations. To do so, Fe_5C_2 nanoparticles of elevated Fe concentrations (0 – 0.05 mM Fe) were dispersed in 1% agarose gel and scanned on a 7T magnet. For particles of the same coating, there was a clear size effect on the T_2 shortening effect, with larger nanoparticles more efficiently inducing hypointensities. For instance, for phospholipid coated Fe_5C_2 nanoparticles, r_2 values were 342, 385, and 450 $\text{mM}^{-1}\text{s}^{-1}$ for 5, 14, and 22 nm particles, respectively (Figure 2A and Table 2). This size effect is attributed to surface canting caused magnetism drop, which is more severe for particles of smaller sizes [37].

For particles of the same size, we compared the r_2 values to assess the impact from coatings. For ZDS coated Fe_5C_2 nanoparticles, we found that the r_2 values were overall comparable to phospholipid-coated ones (Table 2). With the casein coating, however, we observed striking r_2 increase (>200%) for particles of all the three sizes (Table 2). In particular, the casein-coated 22 nm Fe_5C_2 nanoparticles exhibited an exceptional r_2 of 973 $\text{mM}^{-1}\text{s}^{-1}$ (per Fe basis), which is one of the highest for all T_2 probes reported (Figure 2B).

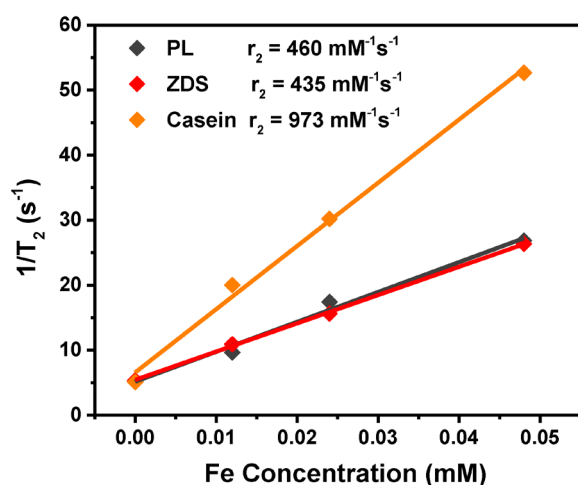


Figure 2: r_2 relaxivity rates of Fe_5C_2 nanoparticles, measured with agarose gel samples containing different concentrations of particles. r_2 values for 22 nm Fe_5C_2 coated with phospholipids, ZDS, and casein. While phospholipids and ZDS coated nanoparticles show comparable r_2 , casein coating increased the r_2 by more than two fold to 973 $\text{mM}^{-1}\text{s}^{-1}$.

Table 2: r_2 relaxivities of Fe_5C_2 nanoparticles of different sizes and surface coatings.

Size (nm)	PL ($\text{mM}^{-1}\text{s}^{-1}$)	ZDS ($\text{mM}^{-1}\text{s}^{-1}$)	Casein ($\text{mM}^{-1}\text{s}^{-1}$)
5	342	338	836
14	385	389	879
22	460	435	973

Cell uptake and cytotoxicity

Cellular uptake and toxicity were studied with RAW264.7 cells (a murine macrophage cell line). Figure 3A shows representative Prussian blue staining images for cells incubated with casein-coated 22 nm Fe_5C_2 nanoparticles of different concentrations (incubation time was 4 h). Clearly, more particles were internalized when the initial particle concentration was increased. When the starting iron content was higher than 20 $\mu\text{g}/\text{mL}$, more than 80% cells in the scope were heavily laden with iron (Figure 3A).

Quantitative cell uptake analysis was performed using inductively coupled plasma-mass spectrometry (ICP-MS). The starting particle concentration was set as 10 $\mu\text{g Fe}/\text{mL}$, and the uptake in pg Fe per cell was compared among formulations of different sizes and coatings. For particles of the same size, no significant difference in uptake was found among the three coatings (Figure 3B). Meanwhile, the particle size has some but no dramatic impact on the cell uptake. Taking casein coated Fe_5C_2 nanoparticle for instance, 22 nm Fe_5C_2 nanoparticles exhibit an uptake of 13.86 pg Fe/cell, compared to that of 13.05 and 10.55 pg Fe/cell for the 14 nm and 5 nm ones, respectively (Figure 3B). This level of Fe loading is in general comparable to that observed with Fe_3O_4 nanoparticles [16]. The nanoparticles induced comparable or even slightly enhanced contrast ability within cells (Figure S4).

Despite of the high iron loading, the cells remain overall healthy. Even at 100 $\mu\text{g Fe}/\text{mL}$, cells maintained ~ 90% viability, regardless of the size and coating (Figures 3B&3C). Notably, in surface modification, we took extra washing steps to remove residual CTAB from the synthesis (Experimental section). That, we believe, is responsible for the increase of cell tolerance relative to what was reported by us previously [15].

in vivo MRI

Based on the cell uptake and relaxivity results, it is determined that casein-coated Fe_5C_2 nanoparticles are the most promising contrast probes. We next set out to investigate these nanoparticles' *in vivo* performances in healthy nude mice. All three size (5, 14, and 22 nm) casein-coated Fe_5C_2 nanoparticles were intravenously (i.v.) injected (2.5 mg Fe/kg, n = 3). Sagittal T_2 -weighted MR images were acquired before and 1 and 4 h after the injection (Figure 4A). For comparison, casein coated 15 nm IONPs were injected as a control (Ocean Nanotech Inc, r_2 was 268 $\text{mM}^{-1}\text{s}^{-1}$, Figure S5A&B). In all animal groups, a significant drop of signal intensity was observed in the liver at 1 h after injection. The hypointensities were maintained but less prominent at 4 h. To quantitatively analyze the

signal change caused the nanoparticles. Specifically, we calculated the change in T_2 ($\Delta T_2\%$) using the equation $\Delta T_2\% = (T_{2pre} - T_{2post}/T_{2pre}) * 100\%$. For Fe_5C_2 nanoparticles, there was a clear size effect on the hypointensity induced, with $\Delta T_2\%$ at 1 h being $43.9 \pm 1.4\%$, $70.8 \pm 1.7\%$, and $82.9 \pm 1.8\%$, respectively, for 5, 14, and 22 nm Fe_5C_2 particles, and $37.9 \pm 0.9\%$, $62.6 \pm 1.1\%$, and $73.3 \pm 1.0\%$ at 4 h. All the three formulations outperformed Fe_3O_4 nanoparticles, which showed a $\Delta T_2\%$ of $48.8 \pm 1.0\%$ and $33.1 \pm 0.7\%$ for the 1 h and 4 h time points, respectively (Figure 4B). The enhanced contrast effect was mostly attributed to the high r_2 of the Fe_5C_2 nanoparticles. After the 4 h imaging, we euthanized the animals and performed Prussian blue staining with tissue samples. There was a large amount of particles accumulated in the liver and spleen, which was attributed to the particle uptake by K upffer cells and splenocytes. Interestingly, for 5 nm Fe_5C_2 nanoparticles, extensive positive staining was observed in the kidneys (Figure 4C). This is attributed to the relatively small size of the particles and indicates possible renal clearance of them. Meanwhile, no detectable damage to the tissues was observed.

Discussion and Conclusion

With high magnetization and good stability in ambient conditions, Fe_5C_2 nanoparticles hold great promise as a novel type of MRI contrast agent for liver imaging. To this end, it is important to optimize the size and surface features of the particles so as to achieve desired contrast ability, toxicity, relaxivity,

and macrophage uptake. In the present study, we modified the synthetic approach to prepare Fe_5C_2 nanoparticles of different sizes. Based on the consideration that there is a layer of iron oxide shell on the Fe_5C_2 core, we adopted three surface modification methods used previously for IONPs to modify Fe_5C_2 nanoparticles. We showed that all the three methods are adequate to grant Fe_5C_2 nanoparticles with good aqueous stability. The size and coating have varied levels of impact on the particles' size, cellular uptake, *in vivo* contrast abilities, and in particular, their r_2 relaxivity. These observations provide useful information for future engineering of Fe_5C_2 nanoparticles for either diagnosis or therapy purposes.

The *in vivo* MRI studies confirm the advantages of Fe_5C_2 nanoparticles over IONPs in the liver imaging. At the same Fe concentration, Fe_5C_2 nanoparticles can more efficiently induce hypointensities to the liver, which is mainly attributed to the high r_2 relaxivity. An interesting observation is the accumulation of 5 nm Fe_5C_2 nanoparticles in the kidneys. This suggests possible renal clearance of Fe_5C_2 particles of small sizes, which may serve as an advantage in other imaging applications. For instance, for targeted cancer imaging, it is preferred that the unbound nanoparticles are rapidly cleared from the host [38]. In this scenario, the 5 nm Fe_5C_2 nanoparticles, which provide comparable relaxivity but efficient renal clearance, may be a better option than the 22 nm formulation. This possibility will be assessed in our future studies.

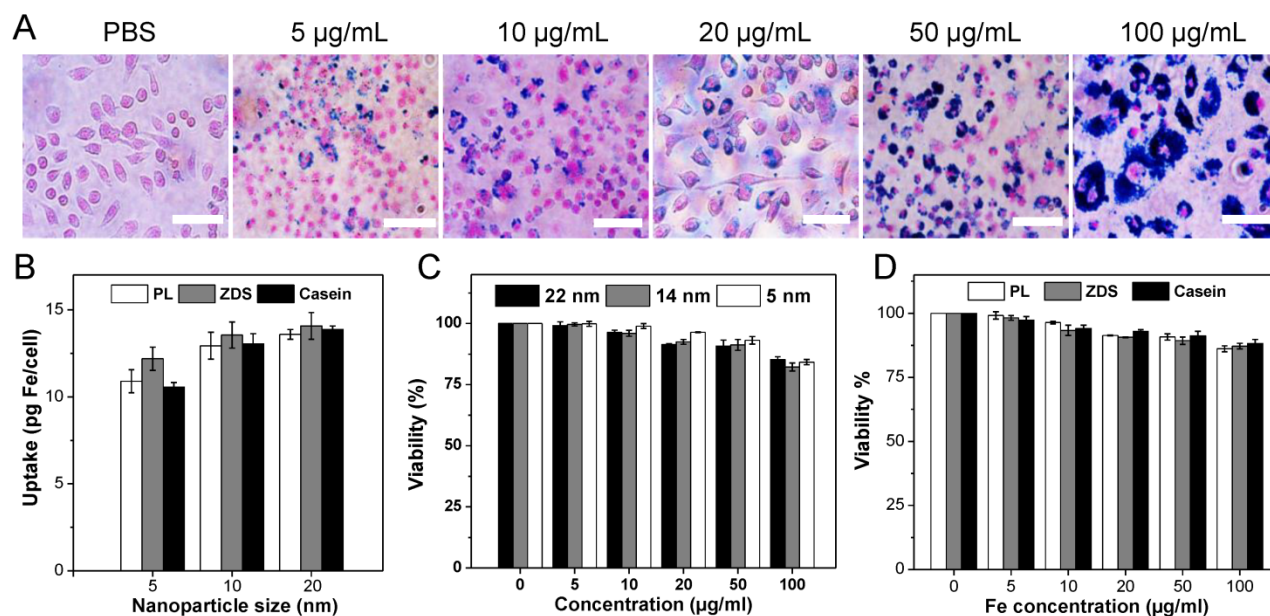


Figure 3: Cellular uptake and cytotoxicity studies. A) Representative Prussian blue staining images of RAW264.7 cells labeled with casein coated Fe_5C_2 nanoparticles. The starting particle concentration was increased from 0 to 100 $\mu\text{g Fe/mL}$ and the incubation lasted for 4 h. Scale bars: 100 μm . B) Quantitative cell uptake data, measured by ICP-MS. The starting concentration was 50 $\mu\text{g/mL}$. The uptake was slightly higher for 22 nm nanoparticles. Meanwhile, little difference was observed among particles of the same core size but different coatings. C) MTT assays with phospholipid coated Fe_5C_2 nanoparticles using RAW264.7 macrophages. The cells retained over 85% viability at the tested concentrations (0 – 100 $\mu\text{g Fe/mL}$). D) MTT assays with 22 nm Fe_5C_2 nanoparticles of different coatings. Comparable viability was observed among the three coatings. All of the formulations showed over 85% viability in the tested concentrations.

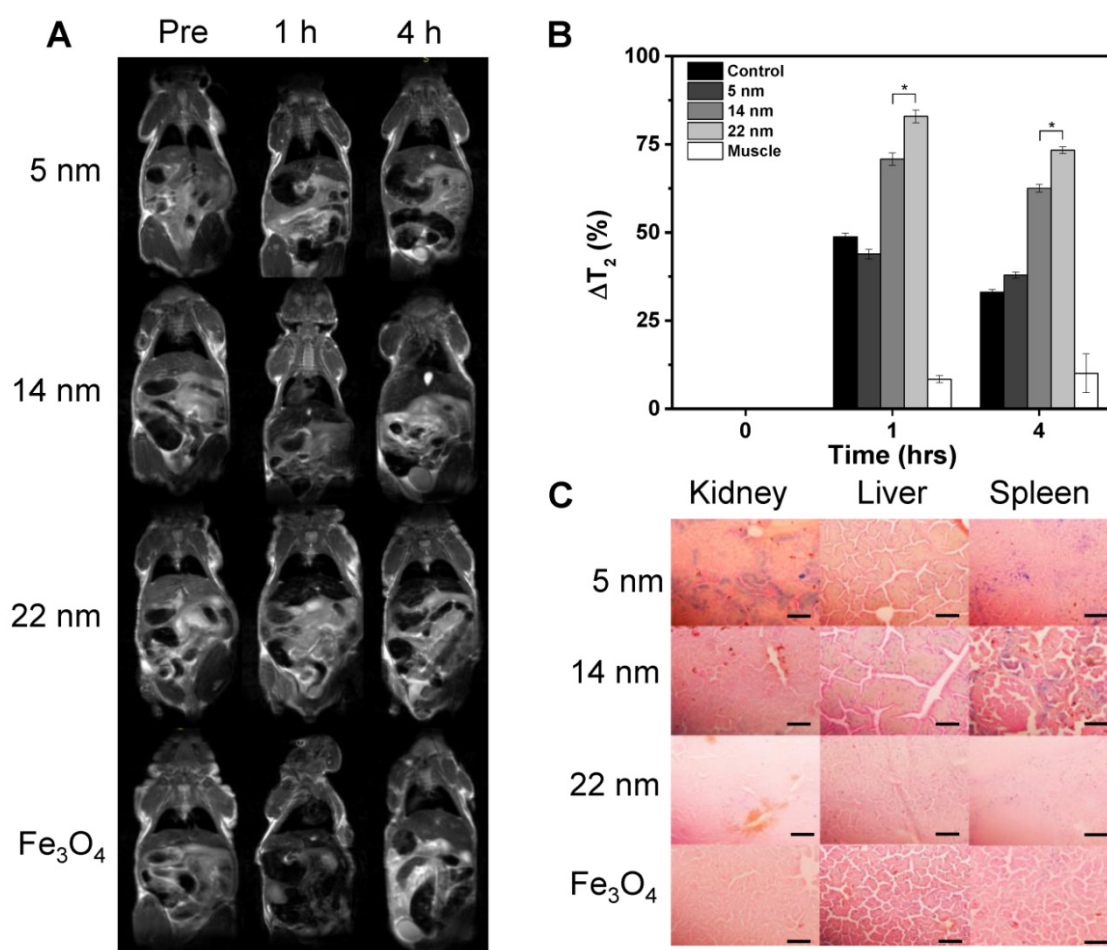


Figure 4: MR imaging and in vivo particle distribution. A) MR imaging results. Normal athymic nude mice were intravenously injected with casein-coated Fe₃C₂ (5 nm, 14 nm, 22 nm) or casein-coated 20 nm Fe₃O₄ nanoparticles. MRI scans were performed on a 7T magnet pre- and 1 hr, and 4 hrs after the injection. Darkening of livers appear prevalent in all the animals. The 22 nm Fe₃C₂ exhibited the most significant contrast among all of the formulations. B) Quantification of liver contrast changes. 14 and 22 nm Fe₃C₂ nanoparticles induced more significant signal drop in the liver than Fe₃O₄ nanoparticles did at 1 and 4 h time points (*P < 0.05). C) Prussian blue staining with tissue samples from the liver, kidney, and spleen. Positive staining was found across the liver and spleen. For 5 nm Fe₃C₂ nanoparticles, positive staining was also found in the kidneys, which was likely attributed to the small size of the particles. Scale bars, 10 μm.

The exceptionally high r_2 relaxivity of Fe₃C₂ nanoparticles is intriguing. By definition, T₂ contrast agents interact with nearby water molecules by inducing a local magnetic field in which the transverse relaxation (T₂) of water is shortened. This manifests as a relatively “dark” area on T₂ weighted images. The outer-sphere relaxivity, which describes the relaxation behavior of water molecules surrounding the contrast agents, is one of the most important contributors to MRI contrast. According to the outer-sphere model of transverse relaxation [39], the r_2 relaxivity is proportional to particle magnetization (M) [40, 41]. This explains the high r_2 of Fe₃C₂ nanoparticles relative to IONPs. For Fe₃C₂ nanoparticles of the same coating, there was a clear size effect on r_2 . This is attributed to the surface canting effect which was previously observed with IONPs [37]. A more interesting observation is a dramatic r_2 increase found with casein coated nanoparticles. This is attributed to the impact of the casein coating on the water diffusion correlation time

(τ_D), which is also proportional to r_2 [42]. Casein is essentially a family of phosphoproteins consisting of four members, αS₁, αS₂, β, and κ caseins. κ-casein, which is the most soluble variant of the four, is believed to play a most contributing role to the enhanced r_2 . It is known that κ-casein has a unique, elongated “hair-like” structure [43]; when coated onto nanoparticles, κ-casein may form a protein layer presenting long, hydrophilic channels, which enable water molecules to come in and interact with the inner water layer that is close to particle surface. The abundant surface hydroxyl and amides of casein may help promote fast proton exchange with water molecules. Meanwhile, the protein coating increases the overall particle size and restricts fast water diffusion. These factors all together lead to an enhanced τ_D, leading to increase of apparent r_2 . More investigations are under way to further elucidate the surface impact of casein, and hopefully, to guide the future design and engineering of magnetic probes with high r_2 re-

laxivity.

Overall, we have prepared Fe₅C₂ nanoparticles of different sizes and surface coatings. We found that both size and surface have an impact on the particles performance as T₂ contrast agents. In particular, with casein coated 22 nm Fe₅C₂ nanoparticles, we observed a striking r₂ of 973 mM⁻¹s⁻¹, making it one of the highest reported T₂ contrast agents to date. The particles showed low toxicity and they outperformed IONPs in inducing hypointensities to the liver. These observations confirm the great potential of Fe₅C₂ nanoparticles as a novel type of MRI contrast agents.

Supplementary Material

Figures S1-S5. <http://www.thno.org/v05p1225s1.pdf>

Acknowledgments

We thank Pradiḡ Basnet from Dr. Yiping Zhao's group for his assistance in XRD analysis. The research was supported by an NCI/NIH R00 grant (R00CA153772, J.X.), an Elsa U. Pardee Foundation Award (J.X.), and a UGA-GRU seed grant (J.X.).

Competing Interests

The authors have declared that no competing interest exists.

References

- Siegel RL, Miller KD, Jemal A. Cancer statistics, 2015. *CA: a cancer journal for clinicians*. 2015; 65: 5-29.
- [Internet] Howlader NN, Krapcho M, Garshell J, et al. SEER Cancer Statistics Review, 1975-2011. http://seer.cancer.gov/csr/1975_2011/
- Ba-Ssalamah A, Uffmann M, Saini S, et al. Clinical value of MRI liver-specific contrast agents: a tailored examination for a confident non-invasive diagnosis of focal liver lesions. *Euro Radiol*. 2009; 19: 342-57.
- Cheon J, Lee JH. Synergistically integrated nanoparticles as multimodal probes for nanobiotechnology. *Accounts Chem Res*. 2008; 41: 1630-40.
- Perilongo G, Shafford EA. Liver tumours. *Eur J Cancer*. 1999; 35: 953-8; discussion 8-9.
- Sherman M. Surveillance for hepatocellular carcinoma. *Best Pract Res Cl Ga*. 2014; 28: 783-93.
- Thian YL, Riddell AM, Koh DM. Liver-specific agents for contrast-enhanced MRI: role in oncological imaging. *Cancer imaging*. 2013; 13: 567-79.
- Longmaid HE, 3rd, Dupuy DE, Kane RA, et al. Noninvasive liver imaging: new techniques and practical strategies. *Semin Ultrasound CT*. 1992; 13: 377-98.
- Van Beers BE, Daire JL, Garteiser P. New imaging techniques for liver diseases. *J Hepatol*. 2015; 3: 690-700.
- Issadore D, Min C, Liang M, et al. Miniature magnetic resonance system for point-of-care diagnostics. *Lab Chip*. 2011; 11: 2282-7.
- Pouliquen D, Le Jeune JJ, Perdrisot R, et al. Iron oxide nanoparticles for use as an MRI contrast agent: pharmacokinetics and metabolism. *Magn Reson Imaging*. 1991; 9: 275-83.
- Li L, Jiang W, Luo K, et al. Superparamagnetic iron oxide nanoparticles as MRI contrast agents for non-invasive stem cell labeling and tracking. *Theranostics*. 2013; 3: 595-615.
- Lee HY, Lee SH, Xu C, et al. Synthesis and characterization of PVP-coated large core iron oxide nanoparticles as an MRI contrast agent. *Nanotechnology*. 2008; 19: 165101.
- Cowger T, Xie J. Polyaspartic acid coated iron oxide nanoprobes for PET/MRI imaging. *Methods Mol Bio*. 2013; 1025: 225-35.
- Tang W, Zhen Z, Yang C, et al. Fe₅C₂ nanoparticles with high MRI contrast enhancement for tumor imaging. *Small*. 2014; 10: 1245-9.
- Xie J, Liu G, Eden HS, et al. Surface-engineered magnetic nanoparticle platforms for cancer imaging and therapy. *Accounts Chem Res*. 2011; 44: 883-92.
- Joshi HM, Lin YP, Aslam M, et al. Effects of shape and size of cobalt ferrite nanostructures on their MRI contrast and thermal activation. *J Phys Chem C, Nanomaterials and interfaces*. 2009; 113: 17761-7.
- Hadjipanayis CG, Bonder MJ, Balakrishnan S, et al. Metallic iron nanoparticles for MRI contrast enhancement and local hyperthermia. *Small*. 2008; 4: 1925-9.
- Liu Y, Yang K, Cheng L, et al. PEGylated FePt@Fe₂O₃ core-shell magnetic nanoparticles: potential theranostic applications and in vivo toxicity studies. *Nanomed-Nanotechnol*. 2013; 9: 1077-88.
- Teng X, Yang H. Iron oxide shell as the oxidation-resistant layer in SmCo₅@Fe₂O₃ core-shell magnetic nanoparticles. *J Nanosci Nanotechnol*. 2007; 7: 356-61.
- Nocera TM, Chen J, Murray CB, et al. Magnetic anisotropy considerations in magnetic force microscopy studies of single superparamagnetic nanoparticles. *Nanotechnology*. 2012; 23: 495704.
- Zhu J, Wu J, Liu F, et al. Controlled synthesis of FePt-Au hybrid nanoparticles triggered by reaction atmosphere and FePt seeds. *Nanoscale*. 2013; 5: 9141-9.
- Horev-Azaria L, Baldi G, Beno D, et al. Predictive toxicology of cobalt ferrite nanoparticles: comparative in-vitro study of different cellular models using methods of knowledge discovery from data. *Part Fibre Toxicol*. 2013; 10: 32.
- Yang C, Zhao H, Hou Y, et al. Fe₅C₂ nanoparticles: a facile bromide-induced synthesis and as an active phase for Fischer-Tropsch synthesis. *J Am Chem Soc*. 2012; 134: 15814-21.
- Tong S, Hou S, Ren B, et al. Self-assembly of phospholipid-PEG coating on nanoparticles through dual solvent exchange. *Nano Lett*. 2011; 11: 3720-6.
- Liu Y, Wang J. Effects of DMSA-coated Fe₃O₄ nanoparticles on the transcription of genes related to iron and osmosis homeostasis. *Toxicol Sci*. 2013; 131: 521-36.
- Wei H, Insin N, Lee J, et al. Compact zwitterion-coated iron oxide nanoparticles for biological applications. *Nano Lett*. 2012; 12: 22-5.
- Quan Q, Xie J, Gao H, et al. HSA coated iron oxide nanoparticles as drug delivery vehicles for cancer therapy. *Mol Pharm*. 2011; 8: 1669-76.
- Wang J, Xie J, Zhou X, et al. Ferritin enhances SPIO tracking of C6 rat glioma cells by MRI. *Mol Imaging Bio*. 2011; 13: 87-93.
- Huang J, Wang L, Lin R, et al. Casein-coated iron oxide nanoparticles for high MRI contrast enhancement and efficient cell targeting. *ACS Appl Mater Interfaces*. 2013; 5: 4632-9.
- Sakulkhu U, Mahmoudi M, Maurizi L, et al. Protein corona composition of superparamagnetic iron oxide nanoparticles with various physico-chemical properties and coatings. *Sci Rep*. 2014; 4: 5020.
- Martin MN, Allen AJ, MacCuspie RI, et al. Dissolution, agglomerate morphology, and stability limits of protein-coated silver nanoparticles. *Langmuir*. 2014; 30: 11442-52.
- Juneja R, Roy I. Surface modified PMMA nanoparticles with tunable drug release and cellular uptake. *Rsc Adv*. 2014; 4: 44472-9.
- Tong S, Hou S, Zheng Z, et al. Coating optimization of superparamagnetic iron oxide nanoparticles for high T₂ relaxivity. *Nano Lett*. 2010; 10: 4607-13.
- Zhao Z, Zhou Z, Bao J, et al. Octapod iron oxide nanoparticles as high-performance T₂ contrast agents for magnetic resonance imaging. *Nat Commun*. 2013; 4: 2266.
- Wei H, Bruns OT, Chen O, et al. Compact zwitterion-coated iron oxide nanoparticles for in vitro and in vivo imaging. *Integr Biol (Camb)*. 2013; 5: 108-14.
- Baaziz W, Pichon BP, Fleutot S, et al. Magnetic Iron Oxide Nanoparticles: Reproducible Tuning of the Size and Nanosized-Dependent Composition, Defects, and Spin Canting. *J Phys Chem C*. 2014; 118: 3795-810.
- Choi HS, Liu W, Misra P, et al. Renal clearance of quantum dots. *Nanotechnology*. 2007; 25: 1165-70.
- Mattoussi H, Cheon J. *Inorganic nanoprobes for biological sensing and imaging*. Boston: Artech House; 2009.
- Gillis P, Koenig SH. Transverse relaxation of solvent protons induced by magnetized spheres: application to ferritin, erythrocytes, and magnetite. *Magn Reson Med*. 1987; 5: 323-45.
- Koenig SH, Gillis P. Transverse relaxation (1/T₂) of solvent protons induced by magnetized spheres and its relevance to contrast enhancement in MRI. *Invest Radiol*. 1988; 23 Suppl 1: S224-8.
- Koenig SH, Kellar KE. Theory of 1/T₁ and 1/T₂ NMRD profiles of solutions of magnetic nanoparticles. *Magn Reson Med*. 1995; 34: 227-33.
- Richardson BC, Creamer LK, Munford RE. Comparative micelle structure. I. The isolation and chemical characterization of caprine kappa-casein. *Biochim Biophys Acta*. 1973; 310: 111-7.